



Response of *Saccharomyces cerevisiae* W303 to Iron and Lead Toxicity in Overloaded Conditions

Gordana Čanadi Jurešić¹ · Božena Ćurko-Cofek² · Martina Barbarić³ · Nermina Mumišić³ · Branka Blagović¹ · Polona Jamnik⁴

Received: 8 September 2020 / Accepted: 7 February 2021 / Published online: 23 February 2021
© The Author(s), under exclusive licence to Springer Science+Business Media, LLC part of Springer Nature 2021

Abstract

Yeast *Saccharomyces cerevisiae* is an ideal model organism for studying molecular mechanisms of the stress response provoked by metals. In this work, yeast cells response to iron (Fe^{3+}) or lead (Pb^{2+}) exposure was tested and compared. Survival test was used to determine testing doses of metal ions—for Fe^{3+} it was 4 mM and for Pb^{2+} 8 mM. These (high, over-loaded) doses provoked comparable values of growth inhibition, but different values in vitality measurement. The percentage of metabolically active cells, determined by fluorescent FUN-1 dye, was lower in Pb^{2+} than in Fe^{3+} treated cells. Besides, endogenous antioxidant defence systems in the cells treated with Pb^{2+} were less efficient compared to Fe^{3+} . At the mitochondrial level, the effects of metal ions were in correlation with the results of cell metabolic activity. The mitochondrial proteome of Pb^{2+} treated cells showed the domination of protein downregulation. Yeast cells treated either with Fe^{3+} or Pb^{2+} shared 19 common significantly changed proteins. The affected proteins were involved in different cellular process and amongst them only five proteins belong to energy and carbohydrate metabolism, and protein biosynthesis. Based on all obtained results, it is possible to conclude that the effects of Fe^{3+} and Pb^{2+} on yeast cells show rather specific patterns of toxicity and stress response.

Introduction

Numerous metals are used in industrial production and as a consequence, they often end up in the environment, resulting in water and soil contamination [1]. Through the water and soil, metals affect ecosystems and accumulate in the human body damaging different organs, most often respiratory, alimentary, and nervous systems [2]. The mechanisms that cause the damage are diverse and may be direct towards enzyme and protein function, cell cycle and differentiation or DNA repair [3]. One of the common mechanisms is

oxidative stress triggered by high levels of reactive oxygen species (ROS) [4]. It is not yet clear how metals promote oxidative stress. One of their possible targets is mitochondria since they are a major source of endogenous ROS through the electrons leaking from the mitochondrial respiratory chain [5]. Although mitochondria have protective mechanisms for ROS detoxification, if the production of ROS is too high, these mechanisms are not sufficient and result in oxidative stress [6].

Harmful effects of metals arise from the fact that they cannot be degraded in the organism and therefore interfere with different cellular processes important for maintaining cellular homeostasis [7]. Based on their toxicity, we can distinguish two groups of metals: essential and non-essential [8]. Essential metals (like iron (Fe), copper (Cu), and zinc (Zn)) participate as cofactors in essential cellular functions in trace amounts [9]. When their concentrations rise above the threshold, they become toxic. Therefore, the metal levels are monitored and regulated by different proteins engaged in metal trafficking inside the organism [10]. Furthermore, metal toxicity also depends on its uptake mechanisms, intracellular distribution and possible interactions, oxidation state, physicochemical properties, and affinity towards different ligands [3].

✉ Gordana Čanadi Jurešić
gordanacj@medri.uniri.hr

- ¹ Department of Medical Chemistry, Biochemistry and Clinical Chemistry, Faculty of Medicine, University of Rijeka, B. Branchetta 20, 51000 Rijeka, Croatia
- ² Department of Physiology and Immunology, Faculty of Medicine, University of Rijeka, B. Branchetta 20, 51000 Rijeka, Croatia
- ³ Faculty of Medicine, University of Rijeka, B. Branchetta 20, 51000 Rijeka, Croatia
- ⁴ Biotechnical Faculty, University of Ljubljana, Jamnikarjeva 101, 1000 Ljubljana, Slovenia

Fe is an essential micronutrient for all eukaryotes, particularly for humans. It is involved in some of the most important processes in the organism, such as oxygen transport, electron transfer, erythropoiesis, oxidative metabolism and immune responses [11]. Despite its essential role in the human body, there are no effective means of excreting Fe [12]. Therefore, any disturbance in Fe homeostasis can result in Fe deficiency or Fe excess, which generates oxidative stress [13]. In the biological systems, Fe can be in +2 or +3 oxidation states. Hence, it is converted by oxidation from Fe^{2+} to Fe^{3+} and by reduction back to Fe^{2+} . This reaction presents the basis of the oxidative metabolism [14]. At the same time, the redox abilities of Fe are responsible for its participation in potentially harmful reactions. Namely, through the Fenton reaction, Fe^{2+} induces the formation of hydroxyl radical ($\text{OH}\cdot$) from H_2O_2 . This is the beginning of the vicious circle where Fe^{3+} reacts with $\text{OH}\cdot$ and reduces to Fe^{2+} ; Fe^{2+} mediates decomposition of H_2O_2 , especially when the environment inside the cell has pro-oxidant properties (particularly in mitochondria), and more $\text{OH}\cdot$ is produced [15].

Non-essential metals (such as lead (Pb), mercury (Hg), and silver (Ag)) are not necessary for the normal function of the human organism; in contrast, they are toxic even at low concentration [16].

Amongst non-essential metals, Pb exposure is one of the most common [17]. Even though Pb is non-redox metal, it can also induce oxidative stress through the accumulation of ROS or depletion of the antioxidants [18]. Pb realizes its toxicity through the ionic mechanism by replacing monovalent or bivalent cations and thus affects cell metabolism. This mechanism results mainly in the development of neurological deficits. Namely, Pb replaces Ca ions and thus gains the ability to cross the blood–brain barrier. Consequently, Pb affects neurotransmitters [18] and causes some changes in the aging brain, which can contribute to the development of neurodegenerative diseases, such as Alzheimer's and Parkinson's disease [19].

Over time, many organisms developed protective mechanisms against environmental metals toxicity [20]. Amongst them is the yeast, *Saccharomyces cerevisiae*, able to neutralise metal toxicity and survive in different forms of toxic stress [21]. Therefore, yeast is considered an ideal model organism for studying the molecular mechanisms of response to metal-induced stress [20]. Furthermore, since many eukaryotic organisms conserved the mechanisms responsible for protection against metal toxicity, studies on yeast could contribute to elucidate molecular mechanisms in higher eukaryotes [3].

To evaluate the toxic effects of various types of environmental stressors, cell viability testing has been largely used method. Environmental factors exert toxic effects through different cellular mechanisms, which may affect the dividing

ability of the cell, but this process doesn't need to end with cell death. Cells can redirect their metabolic processes to set up appropriate defence mechanisms. After a successful recovery, they can continue to divide [22]. For this reason, cell viability data can lead to misunderstanding of the stressors toxicity, and vitality (cell metabolic activity) determination is a better option.

The effect of environmental changes on an organism can be followed at different levels – at the molecular and cellular level, and at the level of organs and organic systems. Amongst the first detected responses to the environmental changes are those that happened at the level of molecules including change of protein profile. Therefore, changed protein profile can serve as an early biomarker of cell stress exposure before its effect is shown on a higher level. Namely, proteins are key factors of function in the living cells [23].

Yeast cell response to metal exposure was reported as arresting cell cycle progression and adapting the transcriptome, proteome, and metabolome [3]. Less is known how metal ions affect the mitochondrial proteome. Namely, mitochondria represent the metabolic dynamism of the cell and with the proteomic approach a global view of mitochondria in one, single experiment is provided [24]. The high-confidence mitochondrial yeast proteome with absolute quantification and topology, defined by integrative organelle proteomics, consists of 901 proteins whilst in mitochondria and mitochondria-associated fractions there are > 3300 of proteins [25]. Since mitochondria play roles in many cellular processes and diseases [23, 26, 27], investigation at the level of proteins, the key players in that processes, is invaluable.

In this study, in an attempt to further characterize the molecular mechanisms of Fe^{3+} and Pb^{2+} ions toxicity to the yeast *S. cerevisiae* in over-loaded conditions, cell viability and vitality were analysed and intracellular oxidation level was measured. Since mitochondrial proteins are the key players of cell physiology, changes at the mitochondrial proteome level were also investigated.

Material and Methods

Cultivation of Yeast

In this study, *S. cerevisiae* strain (W303a – *MATa* {*his3-11,15 leu2-3,112 ura3-1 trp1-1, ade2-1*}), kindly provided from the Collection of Microorganisms of the Institute of Molecular Biotechnology, University of Technology, Graz, was used. Yeast was precultured at 30 °C for 24 h in YPD medium (2% w/v glucose (Fluka, Germany), 2% w/v peptone (Sigma, USA), 1% w/v yeast extract (Sigma, USA)) and then batch cultured for 20 h in YPD medium inoculated at a starting OD_{600} of 0.2 (cca 5×10^6 cells). A control sample of yeast represents non-treated yeast

cells. Besides, in the research yeast cultivated in a media with metal ions (Fe^{3+} or Pb^{2+}) was also used. *S. cerevisiae* W303, the strain used in this study is *his* mutant, and more sensitive to metal stress. According to Pearce and Sherman [28] each of *his1-his7* mutant strains is unable to grow in the presence of elevated levels of metal ions at nearly neutral pH and growth inhibition by metal salts is pH-dependent. For Fe^{3+} growth is inhibited below pH 4.0, and for Pb^{2+} no there is growth below pH 5.5 and above pH 6.0. For that reason, experimental media pH was carefully set to pH 5.5, using 2 M NaOH. The procedure is very delicate because of possible precipitation and needs to be performed very carefully. Culture growth in liquid media was determined by counting the yeast cell number in Bürker-Türk counting chamber (Brand™, Germany).

Determination of Testing Dose (Survival Test)

Over-night cultures of yeast were diluted in liquid YPD to OD_{600} 0.8 (cca 3×10^7 cells) at 30 °C. The exponentially growing yeast cells were then spotted in tenfold dilutions onto solid YPD containing increasing concentration of Fe^{3+} (added in a form of 1 M FeCl_3 solution) or Pb^{2+} (added in a form of 1 M $\text{Pb}(\text{NO}_3)_2$ solution), as well as on YPD control plates (with no metals added). The concentrations of metal ions used in this test were in a range of 0.1–32 mM (0.10; 0.56; 1.00, 1.78; 3.00; 4.00; 5.00, 5.62; 8.00; 10.00; 16.00 and 32.00 mM). All plates were incubated for 48 h, and then the spots of yeast were scored visually to determine growth restriction.

Determination of Yeast Cell Viability

The concentrations of metal-ion determined in survival test (for Fe^{3+} 4 mM and for Pb^{2+} 8 mM) were used in further analysis as a testing dose. In all experiments cells were cultured in 500-ml Erlenmeyer conical flasks and total working volume was 200 ml. The initial pH value of the medium was adjusted and then inoculated. The cultures were cultured in a rotary shaker at 160 rpm and 28 °C. Cell viability was measured by counting the yeast cell number in Bürker-Türk counting chamber, at the beginning of batch culturing, and at the end (early stationary phase, after 20 h for the cells treated with metals, and 9 h for non-treated cells). At first, each experiment was performed by counting the cells in the chamber and by determining the number of colony-forming units after appropriate dilution of the culture. Good correlation of results between the two methods was obtained and afterwards only counting the cells in the chamber was performed.

Determination of Yeast Cell Vitality

Metabolic activity was measured by two-color fluorescence dye FUN-1 [2-chloro-4-(2,3-dihydro-3-methyl-(benzo-1,3-thiazol-2-yl)-methylidene)-1-phenylquinolinium iodide] by two methods: a fluorescence microscopy and a fluorescence plate reader, using Live/Dead Yeast Viability Kit (Thermo Fisher Scientific, USA). Test was performed after batch culturing, on cells with and without metal-ion addition. Both methods were assessed following manufacturer's protocols.

For the fluorescence microscopy, Calcofluor White M2R dye was used to stain cell-wall chitin with blue-fluorescence regardless of metabolic state. Metabolically active cells, converted FUN-1 dye from diffusely distributed cytoplasmic dim green stain to red Cylindrical Intra Vacuolar Structures (CIVS). Only metabolically active cells, with intact plasma membrane and preserved metabolic capability, form CIVS whilst dead cells exhibit extremely bright green fluorescence [22]. Cells with intact membranes but with little or no metabolism activity have a red diffuse cytoplasmic fluorescence different from the granular fluorescence of CIVS. In this part, the interpretation of the results differs from the manufacturers and represents an improvement in the interpretation of the results.

Within a tested culture we counted the number of fluorescent cells stained blue, blue with red CIVS, green and red and determined a percent of dead and living cells in total cell number. Metabolically active and inactive cells were examined from at least 400 cells in one biological replicate.

The proportion of dead and living cells was also determined using a fluorescence plate reader by measuring green and red mean fluorescence. The greatest change in the red/green fluorescence ratio indicates the most efficient conversion of dye from green uniform stain to red CIVS structures. The result of this analysis was normalized to optical density of used yeast culture at 600 nm (OD_{600}).

The excitation wavelength of FUN-1 was 488 nm whilst emission wavelengths were 530 nm (green) and 620 nm (red). The excitation and emission wavelengths for Calcofluor White were 385 and 475 nm. Tecan F200 Infinite multiplate reader (Tecan Austria GmbH, Austria) and a fluorescence microscope Olympus BX51 microscope (Olympus, Tokyo, Japan) were used for these analyses.

Determination of Intracellular Oxidation

Intracellular oxidation was estimated by using 2',7'-dichlorofluorescein (H_2DCF) according to the procedure well explained in Zakrajšek et al. [29]. Non-fluorescent H_2DCF is given as 2',7'-dichlorofluorescein diacetate (H_2DCFDA), which easily penetrates the plasma membrane and is esterified inside the cells. Finally, fluorescent

2',7'-dichlorofluorescein (DCF) is produced and determined fluorometrically [30].

The cells from 2-mL cell cultures (metal treated and non-treated) were sedimented by centrifugation ($14,000 \times g$, 5 min), washed with 50 mM K-phosphate buffer (pH 7.8) and resuspended in the 50 mM K-phosphate buffer at 10% (v/v). The ROS-sensing dye H₂DCFDA (Sigma, USA) was added to a final concentration of 10 μ M. After incubation (28 °C, 30 min), the fluorescence of the cell suspensions was measured using the Safire II microplate reader (Tecan Austria GmbH, Austria). The excitation and emission wavelengths of DCF were 488 nm and 520 nm, and the data are expressed as relative fluorescence unit (RFU), normalized to the number of yeast cells. The number of cells was determined by counting the cells in the Bürker-Türk chamber.

Isolation of Mitochondria

Mitochondria were isolated according to the method of Zinser and Daum [31]. The isolation starts with the spheroplasts preparation from the cells grown in YPD media with and without metal ion added, at the end of batch culturing. For this preparation modified method, well explained in Čanadi Jurešić et al. [32] was used. In brief, prepared spheroplasts were homogenized using Dounce tissue grinder (S–pestle) and an ice-cold breakage buffer (0.6 mol/L mannitol, 0.01 mol/L Tris/Cl pH 7.4 and 0.001 mol/L phenyl methane sulphonyl fluoride). After centrifugation ($3600 \times g$, 5 min) the resulting pellet was resuspended in breakage buffer and homogenized. With repeated action the combined supernatants were obtained. After centrifugation ($14,000 \times g$, 10 min) the pellet containing crude mitochondria was obtained. The pellet was resuspended in breakage buffer and centrifuged ($3000 \times g$, 5 min). Mitochondria were isolated from the supernatant by centrifugation ($14,000 \times g$, 10 min) and washed twice with breakage buffer. Pellet was dissolved in a small amount of buffer and stored at -80 °C.

Preparation of Samples for 2-D Electrophoresis

In isolated mitochondria, after centrifugation ($9000 \times g$, 20 min) and precipitation, Lysis buffer (7 mol/L urea, 2 mol/L thiourea, 4% w/v CHAPS) and protease inhibitors (1% of Lysis buffer amount) were added and incubated for 1 h on ice and occasionally shaken. Samples were centrifuged ($14\,600 \times g$, 1 h) and supernatants (protein extracts) used for further analysis.

Determination of Protein Concentration

The mitochondrial protein concentrations were determined by the method of Bradford [33] using bovine serum albumin (Sigma, USA) as standard.

Two-Dimensional Electrophoresis (2-D Electrophoresis)

The 2-D electrophoresis was performed according to Görg [34], with minor modifications well explained in the Zakrajšek et al. [29]. Briefly, 100 μ g of protein samples were mixed with rehydration solution and applied to 13-cm pH 4 to 7 IPG strips (GE Healthcare, USA). After rehydration the isoelectric focusing was carried out at 20 °C on a Multiphore II system (GE Healthcare, USA). The second dimension (SDS polyacrylamide gel electrophoresis) was carried out with the 12% running gels on a vertical SE 600 discontinuous electrophoretic system (Hoefer Inc, Austria). The 2-D gels were stained with SYPRO Ruby (Invitrogen, Thermo Fisher Scientific, USA). For each sample, three 2-D gels were run under the same conditions.

Protein Visualisation and Image Analysis

2-D gels were documented using a CAM-GX-CHEMI HR system (Syngene, India). 2-D Dymension software, version 2.02 (Syngene, India) was used for gel image analysis. Three gels for each sample were matched to provide an average gel sample. The spots were revealed and quantified based on their normalised volumes. Expression changes (fold changes) were considered as significant if the intensity of the corresponding spot reproducibly differed by more than 1.5-fold in a normalised volume as a comparison between the control and treated samples, and if this was statistically significant (One-Way ANOVA test, $P < 0.05$).

Protein Identification

Spots of interests were cut from the 2-D gel and uncoloured overnight at 25 °C using a destained solution (glacial acetic acid: methanol: dd H₂O = 10%:40%:50%, v:v:v). It was followed by trypsin digestion (10 μ g/mL of Trypsin, Merck, Germany, for 18 h), extraction of digested proteins from gels (with 5% trifluoroacetic acid: acetonitrile = 1:1, v:v) and their purification (using Assay MAP cartridges C₁₈ and Assay MAP BRAVO, Agilent Technologies, USA). In the next steps, the derivatization with α -cyano-4-hydroxycinnamic acid (5 mg/mL in water: acetonitrile = 1:1, v:v) and their spotting onto the MALDI plate were performed. In the last step, peptides were analysed by 4800 Plus MALDI TOF/TOF Analyser (Applied Biosystems, USA). For identification of the peptides, software ProteinPilot v4.5 (Sciex, USA) was used. The software results were combined/compared with *Saccharomyces cerevisiae* NCBI database using Mascot Server [35].

Various protein modifications (deamination, oxidation, and phosphorylation) were also considered.

Statistical Analysis

The data were statistically evaluated using the data analysis software system Statistica, version 13.4.04 (Tibco Software Inc., 2018). The results are shown as mean \pm standard deviation. Differences amongst groups were tested by a non-parametric tests: Mann–Whitney U test or Kruskal–Wallis and post hoc Tukey HSD-test, and the level of significance was set at $P < 0.05$. In the case of identified proteins and fold changes of their expression relative to control (results presented in Table 1; Fig. 5, and S5) the test is One-Way ANOVA, $P < 0.05$, made by 2-D Dymension software, version 2.02 (Syngene, India).

Results

Determination of Testing Dose

Testing doses of metal ions were determined using Survival test. The growth restriction due to the increase of concentration of added metal ion for both tested ions is presented in Fig. 1. The inhibitive effect of Fe^{3+} on biomass growth was dependent on Fe^{3+} concentrations. Fe^{3+} at a concentration of ≥ 5.6 mM inhibited the microbial growth by approximately 100% compared to control. Therefore, the concentration of Fe^{3+} at 4 mM was chosen as a sublethal dose. The inhibitive effect of Pb^{2+} on the biomass growth was not so linearly dependent on the Pb^{2+} concentrations as for Fe^{3+} (Fig. 1). On the contrary, similar growth restriction was noticed in all tested concentrations until the 8 mM of Pb^{2+} concentration. Moreover, at 8 mM colony growth was slow and prolonged (the author's observations). At the concentration of ≥ 10 mM, there was no growth at all. Based on that, the concentration of 8 mM was chosen as a sublethal dose for Pb^{2+} .

Determination of Vitality and Viability

According to viability test measured by counting yeast cells at the beginning and at the end of batch culturing (until the cells reach early stationary phase), differently treated yeast cells had comparable values of growth inhibition. It was 96% for Fe^{3+} treated and 94% for Pb^{2+} treated yeast cells, respectively (Fig S1).

Although a similar effect of both metal ions on yeast viability was observed, differences in vitality were obtained. Percent of metabolically active cells (that form CIVS) with the intact plasma membrane and preserved metabolic capability in relation to the total cell number was lower in Pb^{2+}

treated cells compared to Fe^{3+} indicating the stronger toxic effect of Pb^{2+} on yeast cells (Fig. 2a and b). The results obtained by fluorescent microscopy were confirmed measuring FUN 1 red/green fluorescence ratio in yeast suspension using a microplate reader (Fig. 2c). FUN 1 red/green ratio was significantly lower in both treated samples compared to control. Pb^{2+} treated cells had a significantly lower ratio in comparison to Fe^{3+} treated cells, which was shown as a less efficient dye conversion. Both measuring approaches (microscopic and by microplate reader) correlate well and show a similar pattern.

Determination of Intracellular Oxidation

Since metabolic activity is related to reactive oxygen species (ROS) production [15] we additionally measured intracellular oxidation. Usually, intracellular oxidation is measured at the end of stressor exposure. In this research measurements were taken at 0, 2, 4 and 20 h from metal ions addition, since cellular redox status is a dynamic process dependent on endogenous antioxidant defence systems. The highest intracellular oxidation was observed at $t=0$ values. At later time points of cultivation intracellular oxidation decreased for Pb^{2+} as well as for Fe^{3+} treated cells, but they were still significantly higher compared to the control. At 4 and 20 h, the difference in intracellular oxidation level between Pb^{2+} and Fe^{3+} treated cells was observed with higher values for Pb^{2+} treated cells (Fig. 3). This indicates that endogenous antioxidant defence systems in the cells treated with Pb^{2+} are less efficient leading to oxidative damage of cellular components. Results of intracellular oxidation correspond to results of vitality obtained by fluorescent microscopy or by measuring FUN1 red/green ratio. In both cases, cellular metabolic activity at all time points was lower in Pb^{2+} treated cells compared to Fe^{3+} treatment.






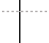





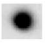












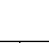








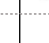

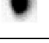
Mitochondrial Proteomic Analysis

Mitochondrial proteome of the cells grown in YPD media with Pb^{2+} or Fe^{3+} and without metal ion added, at the end of batch culturing was detected by 2-D electrophoresis (Table 1; Figs. 4, 5, and S2–S4).

A total of 327 proteins were identified in isolated mitochondria in the control sample, 243 proteins in the mitochondria of yeast treated with Fe^{3+} , whilst the highest content (586 proteins) was found in the mitochondria of yeast treated with Pb^{2+} (Fig. 5).

Correlation of protein expression in both groups of treated cells and in control sample is low ($r^2=0.26$) (Fig. 5). In the case of Pb^{2+} a downregulation of 15 different proteins (18 is actual total number, but protein isomers were also present, A/N) compared to the control was observed. Amongst those 15, 3 proteins were also downregulated in Fe^{3+} treated

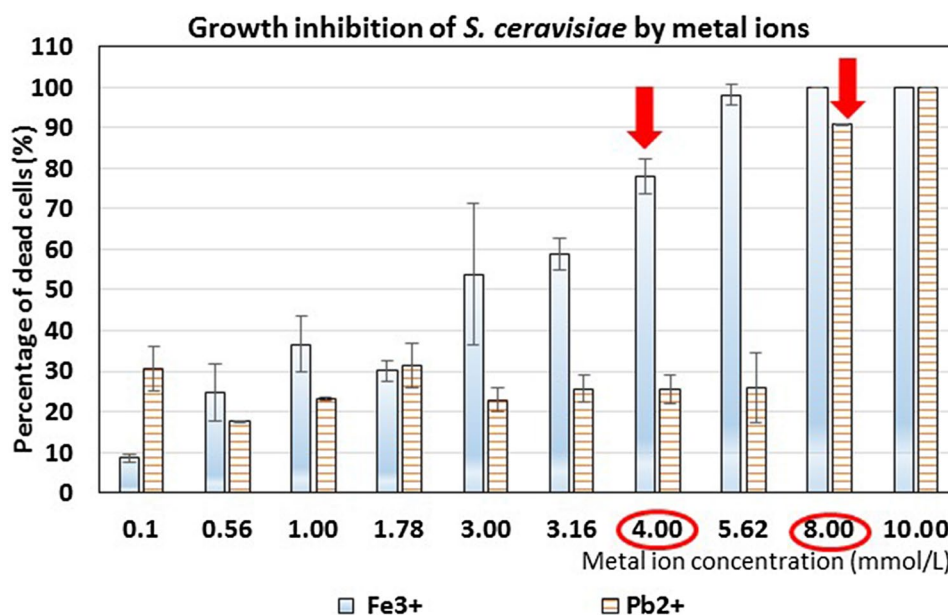
Table 1 Identified proteins and fold changes of their expression in treated yeast cells (Fe^{3+} or Pb^{2+}) relative to control (untreated cells)

Protein Name	<i>p</i> value *	CONTROL		Fe^{3+}	Pb^{2+}
		Norm. Vol. Ratio		Fold changes**	Fold changes**
BIOLOGICAL PROCESSES (GO)					
ATP metabolic processes					
Atp2 - β subunit of the F1 sector of mitochondrial F1F0 ATP synthase	0.003		1	 +1.31	 -5.92
Atp2	0.013		1	 +1.29	 -3.59
Cor1 - Core subunit of the bc1 complex	0.022		1	 -1.23	 -17.58
Cox 6 - Subunit VI of cyt c oxidase	0.013		1	 -1.12	 -6.17
Pda1 $_{\alpha}$ - E1 α subunit of the pyruvate dehydrogenase (PDH) complex	0.027		1	 -3.05	 -4.94
Qcr2 - Subunit 2 of the ubiquinol cytochrome-c reductase complex	0.008		1	 +1.14	 -8.02
Qcr7 - Subunit 7 of the bc1 complex	0.022		1	 -1.34	 -8.14
Tpi1 - Triose phosphate isomerase	0.024		1	 -1.21	 +2.49
Carboxylic acid metabolic process					
Ald4 - Aldehyde dehydrogenase	0.037		1	 -3.14	 -7.15
Cit1 - Citrate synthase	0.005		1	 +1.12	 -3.23
Dld1 - D-lactate dehydrogenase	0.002		1	 -1.05	 -11.67
Lys12 - Homo-isocitrate dehydrogenase	0.045		1	 +8.16	 +3.26
Cell redox homeostasis					
Sco2 - Copper metallochaperone essential for the synthesis and maturation of cyt c oxidase subunit II	0.013		1	 -1.82	 -2.49
Sco2	0.009		1	 -1.94	 -3.98
Tsa2 - Thioredoxin peroxidase	0.010		1	 -1.28	 -2.51
Other					
Eft1 α - Elongation factor 2	0.011		1	 +1.62	 +15.82
Eft1 β - Elongation factor 2	0.003		1	-	 +9.69
Rim1 - ssDNA-binding protein essential for mitochondrial genome maintenance	0.018		1	 -1.39	 -5.69
Tom40 - Component of the TOM (translocase of outer membrane) complex	0.020		1	 +1.23	 -3.35

*In table was shown only statistically significantly different (by One-Way ANOVA test) fold changes of particular proteins ($P < 0.05$) between treated samples (either Fe^{3+} or Pb^{2+}) and control (untreated yeast)

**Protein expression change (fold change up [+]) or down [-])

Fig. 1 Determination of testing dose of metal ions to the *Saccharomyces cerevisiae* cells performed by Survival test: serial dilution-spotting assay to assess the growth of *S. cerevisiae* W303a on YPD medium (set to final pH 5.5) containing either different concentration of FeCl_3 or $\text{Pb}(\text{NO}_3)_2$ (0.10; 0.56; 1.00; 1.78; 3.00; 3.16; 4.00; 5.00; 5.62; 8.00; 10.00). Plates were incubated at 30 °C for 2 days. Mean values of at least three independent experiments are presented



cells, whilst for the remaining 12 proteins a fold change in the context of down- or upregulation was < 1.5 and thus, non-significant.

These common three proteins are: E1 α subunit of the pyruvate dehydrogenase (PDH) complex (Pda1 $_{\alpha}$), aldehyde dehydrogenase (Ald4) and copper metallochaperone essential for the synthesis and maturation of cytochrome c oxidase subunit II (Sco2). Pda1 $_{\alpha}$ and Ald 4 are related to energy and carbohydrate metabolism, whilst Sco2, a protein similar to Sco1p may have a redundant function with Sco1p in delivery of copper to cytochrome c oxidase ([36], Fig S5). If we compare their downregulation between both treated cells, it is more intense in the case of Pb^{2+} , which indicates less efficient processes in Pb^{2+} treated cells. (Table 1; Fig S5). Additionally, Sco2 appeared on 2-D gel in two spots for both metal treatments, which could indicate posttranslational modifications due to treatment. Other proteins, which were downregulated in Pb^{2+} treated cells, belong to different cellular processes such as energy and carbohydrate metabolism (Dld1, Cor1, Qcr7, Cox 6, Atp2, Cit1, Qcr2), transport (Tom40), genetic information processing (Rim1) and oxidative stress response (Tsa2).

Discussion

In this work, yeast cells response to the exposure to one essential metal (Fe) and one toxic metal (Pb) was tested and compared. The inhibitive effect of Fe^{3+} on biomass growth was dependent upon the Fe^{3+} concentrations. The concentration of Fe^{3+} at 4 mM was chosen as a sublethal dose. According to Holmes-Hampton et al. [37] Fe-overload growth conditions are defined to be > 40 μM (Fe_{med}). Although little is

known about the Fe content and distribution in cells grown under these overload conditions, wild type *S. cerevisiae* cells grow reasonably well in medium containing as much as 5–10 mM Fe^{2+} and 20 mM Fe^{3+} . The concentration of Pb^{2+} at 8 mM, determined to be a testing dose, is very high and is surprising given data of literature. According to Chen and Wang [38] the Pb^{2+} at a concentration of 5 μM inhibited the microbial growth by approximately 30% compared to control. Sousa and Soares [39] were used Pb^{2+} concentrations up to 1 mM in their experiments with end-point study at 3 h, whilst Yuan and Tang [40] cultured yeast cells for 72 h at the concentrations of Pb at 1 (11.6 $\mu\text{g}/\text{dl}$) and 8 ppm (92.6 $\mu\text{g}/\text{dl}$). Both tested doses significantly damaged DNA structure of the yeast cells.

According to viability test (Fig S1) differently treated yeast cells had comparable values of growth inhibition (96% for Fe^{3+} and 94% for Pb^{2+} , respectively). Kwolek-Mirek and Zadrag-Tecza [22] explained in detail different methods for viability testing. They accentuated the purpose of viability testing only in the estimation of the degree of growth inhibition, without distinguishing live cells and cells unable to reproduce. Many toxic effects of chemical or physical factors do not lead directly to cell death. Instead, they may cause a numerous physiological (morphological, intracellular, or metabolic) changes resulting in the dividing inability, yet the cell itself may still be alive. For this aspect cell vitality has to be measured. Metabolic activity, as one of the vitality methods, includes the yeast-specific dye FUN-1 [22]. The dye makes it possible to distinguish live (metabolically active), metabolically weakened, and dead cells using fluorescence microscopy and spectrometry. Although a similar effect of both metal ions on yeast viability was observed, differences in vitality were obtained. Percent of metabolically active

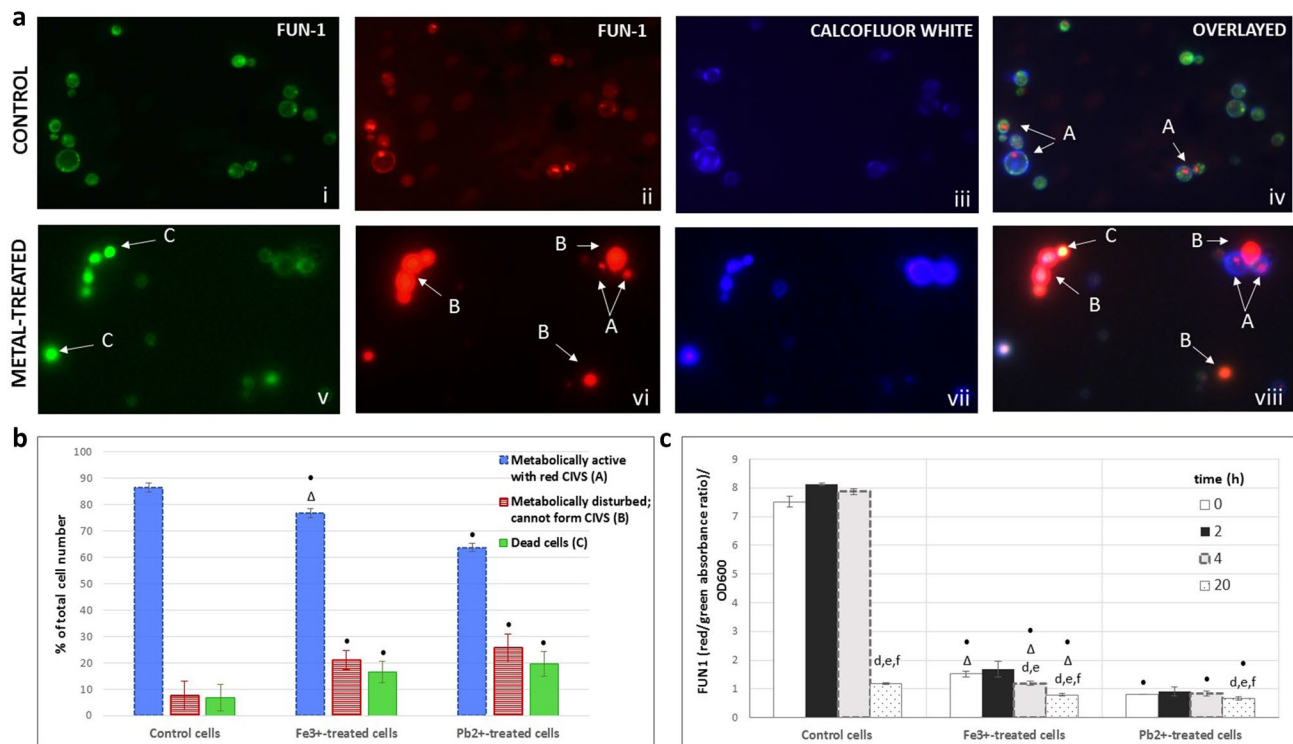


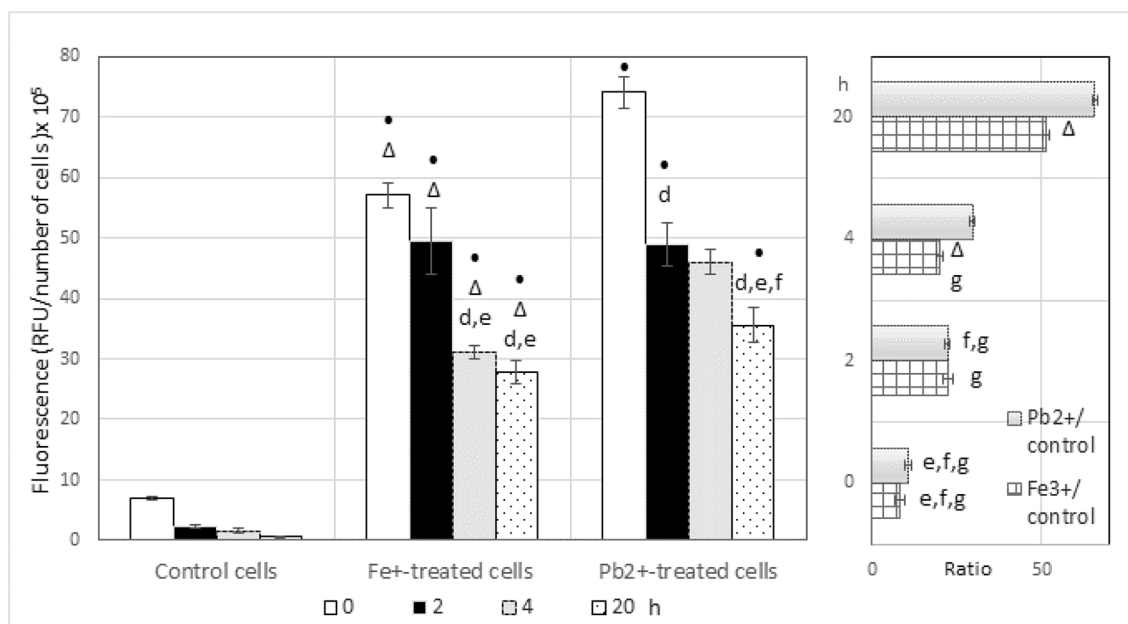
Fig. 2 Assessment of the metabolic activity of the *S. cerevisiae*. (a) Representative fluorescence micrographs of control (i, ii, iii, iv) and metal-treated yeast cells (v, vi, vii, viii) stained with combination of FUN-1 dyes (i, ii, v, vi) or Calcofluor white M2R (iii, vii), and overlaid images (iv, viii). Metabolically active cells form red fluorescent cylindrical intravacuolar structures (CIVS) (a). Cells with intact membranes but with little or no metabolic activity have diffuse red cytoplasmic fluorescence and no CIVS (b). Dead cells show extremely bright, diffuse green fluorescence (c) (magnification 1000 \times). (b) Metabolic activity determined using Live/Dead Yeast Viability Kit by a microscopy. FUN-1 and Calcofluor white M2R fluorescence was examined under the fluorescence microscope using at least 400 cells in each experiment. The result is expressed as relative ratio (%) of blue cells with red CIVS, red and green cells in total cells. Bars indicate SD, $P < 0.05$, Mann–Whitney U test. Symbol \bullet indicates significant differences between control vs. metal-

ions treated cells, whilst Δ indicates significant difference between Fe³⁺-treated cells vs. Pb²⁺-treated cells. (c) Metabolic activity determined using Live/Dead Yeast Viability Kit by a microplate reader. The proportion of living and dead cells was measured, expressed as ratio of red and green absorbance, normalized to the OD₆₀₀. Test was performed in metal-treated cells and control cells in four time intervals (at the beginning of the experiment-time 0, after 2 and 4 h of exposure to metal-ions and at the end of the experiment). Bars indicate SD, $P < 0.05$, Kruskal–Wallis and Post Hoc-Tukey HSD test. Symbol \bullet indicates significant differences between control vs. metal-

cells in relation to the total cell number was lower in Pb²⁺ treated cells compared to Fe³⁺ indicating the stronger toxic effect of Pb²⁺ on yeast cells (Fig S1). Millard et al. [41] explained that during FUN-1 processing a cytosolic reaction with reduced glutathione (GSH) proceeds and glutathione conjugates are formed. Further biochemical modification is necessary, then dye is transported and sequestered in the vacuole, and CIVS are formed. Besides, in the detoxification of several metals the involvement of GSH and vacuole is described (explained in [42]). GSH form complexes with metals (less metal is available for toxic interaction) whilst vacuoles are place for metal sequestration or metal compartmentalization (less metal is present in the cytosol). Considering results obtained in this work, the inhibition of CIVS formation in both treatments may suggests that

in detoxification of both metals, both of above mentioned mechanisms could be involved. Similar implications are found for Pb in the research of Van der Heggen et al. [42] at even lower applied toxic concentrations.

According to obtained results of mitochondrial proteome of the cells grown in YPD media with and without Pb²⁺ or Fe³⁺ addition (Table 1; Figs. 4 and 5) the highest content of proteins was found in the mitochondria of yeast treated with Pb²⁺. Mitochondria have a major role in controlling H₂O₂ and consequently in redox regulation. They export metabolic components which provide signalling for metabolites which support switching mechanisms to control the structural and functional organization of proteins and dictate the control of gene expression [43]. According to Hosiner et al. [21] a part of general detoxification mechanisms to acute metal



Small letters or symbols indicate statistical difference (Kruskal-Wallis and Post Hoc-Tukey HSD test, $p < 0.05$) as follows:

- indicates significant differences between control vs. metal-ions treated cells
- Δ indicates significant difference between Fe³⁺-treated cells vs. Pb²⁺-treated cells
- d - Significantly different comparing time 0 h, the same treatment
- e - Significantly different comparing time 2 h, the same treatment
- f - Significantly different comparing time 4 h, the same treatment
- g - Significantly different comparing time 20 h, the same treatment

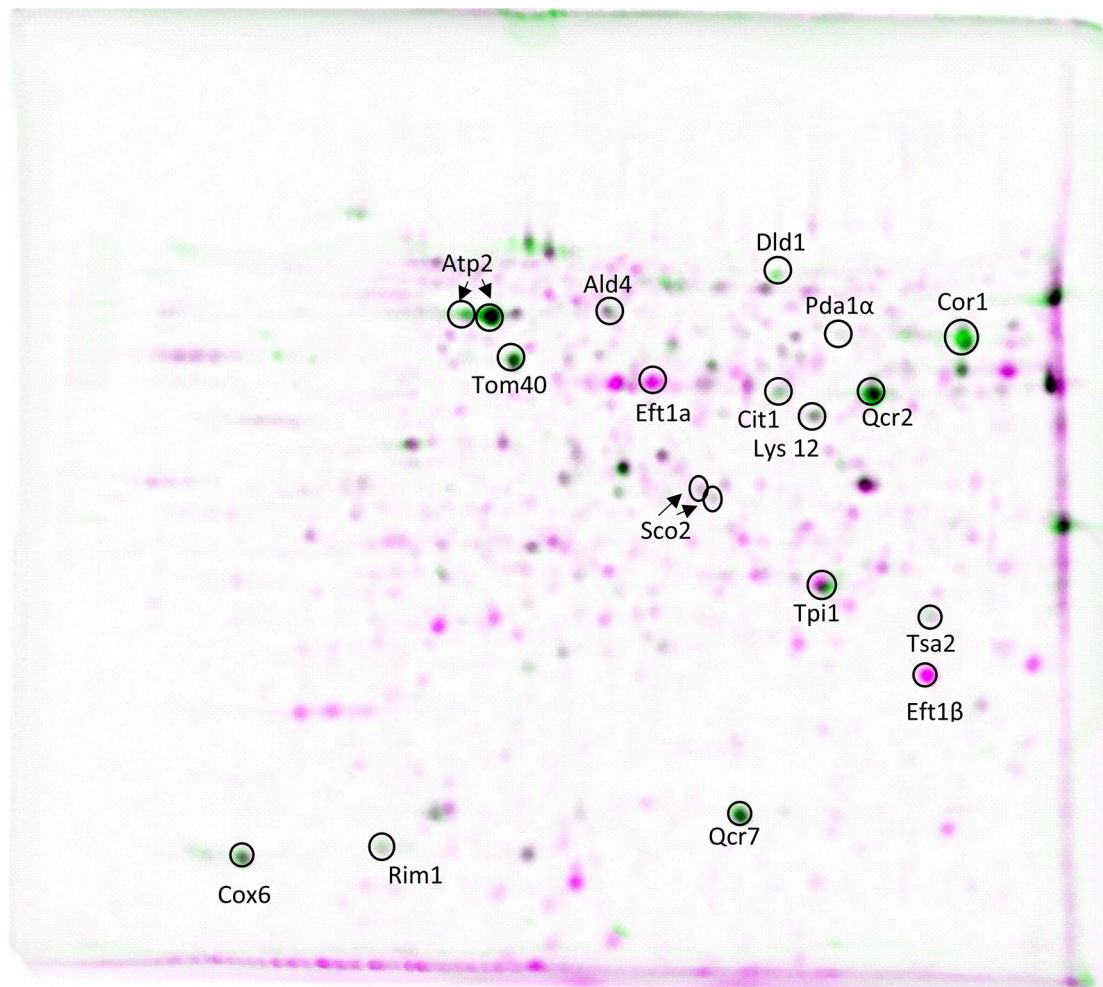
Fig. 3 Intracellular oxidation of *Saccharomyces cerevisiae* yeast cells treated either with Fe³⁺ or Pb²⁺ ions and compared to the control sample, expressed as relative fluorescence unit (RFU)/number of cells $\times 10^5$. Measurements were obtained immediately after metal ions addition (time zero) and 2, 4 and 20 h after metal ions addition. In the

right part of picture relative values of ratios (Fe³⁺/control and Pb²⁺/control) are presented. Quantities indicate the average of at least three independent experiments. Error Bars indicate SD, $P < 0.05$, Kruskal-Wallis and Post Hoc-Tukey HSD test

toxicity in yeast is the induction of genes coding for chaperones and those for chelation of metal ions via siderophores and amino acids. It was shown that yeast cells adapt to oxidative stress by altering global transcription [44]. This can result in increased protein synthesis because of the need for antioxidant enzymes and free radical scavengers [45]. On the other hand, it can also lead to the inhibition of protein synthesis [46]. Experimental data show that high H₂O₂ treatment causes a slower rate of ribosomal runoff, increases the average mRNA transit time, and inhibiting the protein synthesis [44].

More intense response in Pb²⁺ treated cells is also visible in greater number of significantly downregulated proteins, comparing Fe³⁺ treated cells. A reduced abundance of proteins in Pb²⁺ treated cells could be due to decreased import of proteins into mitochondria. One of these downregulated proteins is Tom40, the central component of the translocase of the outer mitochondrial membrane (TOM complex) providing the central protein entry gate

for virtually all precursor proteins. Though mitochondria possess their own genome and translation machinery, only a small number of mitochondrial proteins are encoded by mtDNA and synthesized within the organelle [43]. The coding capacity of the *S. cerevisiae* mitochondrial genome is typical of most modern eukaryotes. It encodes only seven essential components of three respiratory chain complexes: complex III, complex IV and complex V, the complete set of 24 tRNAs required for translation, both ribosomal RNAs—and the 9S RNA component of RNase P. Thus, most proteins is nuclear-encoded and have to be imported into mitochondria through Tom complex [25, 43, 47]. According to results presented in Table 1, Tom40 shows a 3.3-fold reduced amount in Pb²⁺ treated cells compared to the control, whilst in Fe³⁺ treated cells a fold change is not significant. Thus, import of precursor proteins into mitochondria is limited in Pb²⁺ treated cells indicating less efficient processes such as the activity of the mitochondrial electron transport chain complexes,



Pink colored spots – treatment with lead; green spots – treatment with iron.

Legend: **Ald4** - aldehyde dehydrogenase; **Atp2** - β subunit of the F1 sector of mitochondrial F1F0 ATP synthase; **Cit1** - Citrate synthase; **Cor1** - Core subunit of the bc1 complex; **Cox 6** - Subunit VI of cyt c oxidase; **Dld1** - D-lactate dehydrogenase; **Eft1 α** and **1 β** - Elongation factor 2; **Lys12** - Homo-isocitrate dehydrogenase; **Pda1 α** - E1 α subunit of the pyruvate dehydrogenase (PDH) complex; **Qcr2** - Subunit 2 of the ubiquinol cytochrome-c reductase complex; **Qcr7** - Subunit 7 of the bc1 complex; **Rim1** - ssDNA-binding protein essential for mitochondrial genome maintenance; **Sco2** - Copper metallochaperone essential for the synthesis and maturation of cyt c oxidase subunit II; **Tom40** - Component of the TOM (translocase of outer membrane) complex; **Tpi1** - Triose phosphate isomerase; **Tsa2** - thioredoxin peroxidase;

Fig. 4 Representative overlapped 2D-gel. The horizontal axis is the isoelectric focusing dimension, which stretches from pH 4 (left) to pH 7 (right). The vertical axis is the PAGE dimension, which stretches from about 15 kDa (bottom) to at least 120 kDa (top)

substrate oxidation through the tricarboxylic acid cycle and ATP synthesis. This is sustained by the downregulation of proteins involved in ATP metabolic processes (such as Atp2, Cor1, Qcr2, Qcr7 and Pdh7, Table 1) in Pb^{2+} treated cells. Thus, proteomic results show a similar pattern to the results of vitality and intracellular oxidation (Figs. 2, 3, and S1). Additionally, the mitochondrial genome is also affected, since Rim1—a single-stranded DNA-binding protein, which is essential for mitochondrial genome maintenance and involved in mitochondrial DNA replication [36] is downregulated by 5.7-fold compared to the control. Additionally, downregulation of thioredoxin peroxidase (Tsa2) related to cellular antioxidant defence

system indicates less efficient oxidative stress response in Pb^{2+} treated cells and consequently higher oxidation level, compared to Fe^{3+} .

Downregulation of energy and carbohydrate metabolism-related enzymes in treated cells is consistent with the results obtained in Justinić et al. [48] and in Shi et al. [49], resulted in lipid accumulation and is one of the yeast response to stress. In order to ensure enough acetyl-CoA, which is the precursor for fatty acids, yeast ensures downregulation of the majority of glycolytic, gluconeogenesis and TCA cycle enzymes.

Besides, in this research, in both treated yeasts, mitochondrial polar lipids significantly increased comparing control

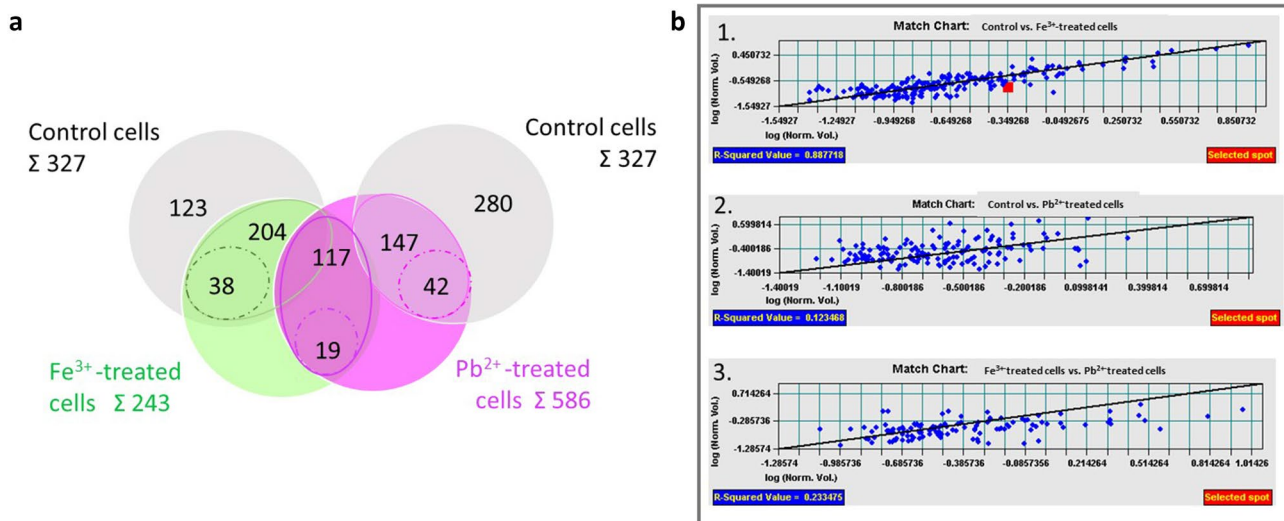


Fig. 5 **a** Schematic diagram of detected proteins in the control and treated yeast cells (One-way ANOVA, $P < 0.05$). Number of overlapped proteins, showing significant difference is indicated with dashed line. **b** Correlation (One-Way ANOVA, $P < 0.05$) between

protein expression in: 1. control cell vs. cells treated with Fe³⁺ ions. 2. control cell vs. cells treated with Pb²⁺ ions. 3. cells treated with Fe³⁺ ions vs. cells treated with Pb²⁺ ions

sample (data not shown), emphasizing the necessity of lipids crosstalk and rearrangement. Sufficient energy supply and suitable protein-lipid construction are necessary for optimal mitochondrial work [50].

Recent studies revealed that mitochondrial homeostasis and function are substantially dependent on a direct adjustment of the activity of the mitochondrial protein import machinery [43, 47]. Decreased import of precursor proteins into mitochondria could be one reason for the downregulation of the aforementioned proteins. Since higher intracellular oxidation was observed in Pb²⁺ treated cells compared to Fe³⁺, decreased protein expression may be a result of ROS induced oxidative damages of proteins, including Tom40. Based on metabolic activity in Pb²⁺ treated cells, it is evident that antioxidant defence systems are less efficient in Pb²⁺ compared to Fe³⁺ treated cells. Damages of proteins involved in the respiratory chain alter its activity resulting in unregulated production of ROS [51].

On the other hand, expression of 4 proteins (amongst them also cytosolic proteins) was increased in cells exposed to Pb²⁺. These were elongation factor 2 (Eft1 α and Eft1 β), triose phosphate isomerase (Tpi1) and homo-isocitrate dehydrogenase (Lys12). Lys12 were overexpressed also in Fe³⁺ treated cells, even more than in Pb²⁺ treated cells whilst Eft1 β wasn't expressed in Fe³⁺ treated cells.

An association of cytosolic glycolytic enzymes with mitochondria in yeast is reported, but their presence is considered to be cytosolic contamination [27, 52]. Nowadays is proposed that such association of proteins may play a functional role in metabolite channelling [25]. Since the cells in both types of treatments faced the oxidative stress, increased

expression of proteins Lys12, Eft1 α and Eft1 β related to providing amino acids and protein biosynthesis was expected. Regarding lysine, it is well known that the genus *Saccharomyces* exhibit an upregulation of the lysine synthesis in response to the oxidative stress [53]. *S. cerevisiae* synthesizes the essential amino acid L-lysine via the L-alpha-aminoadipic acid pathway [54] and one of the enzymes of that metabolic pathway (Lys12) is significantly upregulated. Surprisingly, in our research fold changes of upregulation was greater in Fe³⁺ treated cells than in Pb²⁺ treated cells (Table 1). Lys 12 (homoisocitrate dehydrogenase) oxidises homoisocitrate to 2-oxoadipate, a compound that can be easily transferred to 2-aminoadipate [54]. Still remains an open question if the cell, whilst combating the stress, synthesize Lys precisely or some other by-product of that metabolic pathway. It is known that these yeast cells during exposure to the toxic level of Fe³⁺ and/or Pb²⁺ respond to the stress by dynamic changes in metabolism. The transition from the glycolysis to the pentose phosphate pathway is assumed. Beside glycolysis, in Pb²⁺ treated cells precisely, all further steps of energy gaining processes were repressed, such as oxidative decarboxylation of pyruvate (decreased Pda1 α), TCA cycle (decreased Cit1), pyruvate-acetaldehyde-acetate pathway (decreased Ald4) and oxidative phosphorylation (decreased Cor1, Cox6, Qcr2, Qcr7, Atp2) and even pyruvate—lactate conversion (decreased Dld1). Only for Tpi1 (triose phosphate isomerase), the enzyme responsible for reversible interconversion of the triose phosphate isomers: dihydroxyacetone phosphate and D-glyceraldehyde 3-phosphate, the expression increased, indicating possible gate to the pentose phosphate pathway and NADPH production. NADPH

is particularly important since it provides reducing power for most antioxidants and redox regulatory enzymes. Beside in combating oxidative stress, NADPH is sometimes required for rapid cell growth. In growing cells, there might be less NADPH available for handling accumulated ROS than in non-growing cells. Nielsen [55], based on the research of Olin-Sandoval et al. [53] explained one of the possible ways of handling oxidative stress, using lysine. In the presence of the lysine, yeast cells can allocate more NADPH for dealing with accumulated ROS. Moreover, a possible connection with lysine decarboxylation product, cadaverine and autophagy, and consequent stress protection is found [55]. This is currently an open question and much remains to be discovered.

Conclusion

The results showed the importance of measuring cell vitality and not only cell viability in determining the toxicity of environmental stressors. Although a similar effect of both (over-loaded) metal ions on yeast viability was observed, differences in vitality were obtained. The percentage of metabolically active cells with the intact plasma membrane and preserved metabolic capability according to the total cell number was lower in Pb^{2+} treated cells compared to Fe^{3+} . Furthermore, results of cell metabolic activity were in good correlation with the results of mitochondrial proteome changes. In Pb^{2+} treated cells downregulation of proteins dominated. The most affected proteins arisen from different cellular processes such as energy and carbohydrate metabolism, transport, genetic information processing and oxidative stress response. Amongst all detected 19 proteins, whose expression was changed in the context of up- or downregulation, yeast cells treated with Fe^{3+} or Pb^{2+} shared only five proteins with significant change belonging to energy and carbohydrate metabolism and protein biosynthesis. We found also that one of the targets with decreased expression in Pb^{2+} treated cells is Tom40, which represents the central protein entry gate of precursor proteins into mitochondria. Based on our results providing information about the physiological state of the cells, it possible to conclude that Fe^{3+} and Pb^{2+} exert their toxicity through different molecular mechanisms, inducing different stress response with a less efficient antioxidant defence systems in Pb^{2+} treated yeast cells.

Supplementary Information The online version contains supplementary material available at <https://doi.org/10.1007/s00284-021-02390-3>.

Acknowledgements This work has been supported by University of Rijeka, Project No. 813.10.1113.

Author Contributions Conceptualization, GČJ and PJ; methodology, formal analysis, GČJ, BČC, MB, NM; investigation, GČJ; resources,

BČC; writing—original draft preparation, GČJ and PJ; writing—review and editing, BČC. GČJ; visualization, BČC and GČJ; supervision, PJ and BB; project administration, BB. All authors have read and agreed to the published version of the manuscript.

Funding This work has been supported by University of Rijeka, Project No. 813.10.1113.

Data Availability The authors confirm that the data supporting the findings of this study are available within the article. Any additional data are available from the corresponding author.

Compliance with Ethical Standards

Conflict of interest All authors have declared no competing interests.

References

1. He ZL, Yang XE, Stoffella PJ (2005) Trace elements in agroecosystems and impacts on the environment. *J Trace Elem Med Biol* 19(2–3):125–140. <https://doi.org/10.1016/j.jtemb.2005.02.010>
2. Jan AT, Azam M, Siddiqui K, Ali A, Choi I, Haq QMR (2015) Heavy metals and human health: mechanistic insight into toxicity and counter defense system of antioxidants. *Int J MolSci* 16(12):29592–29630. <https://doi.org/10.3390/ijms161226183>
3. Wysocki R, Tamas M (2010) How *Saccharomyces cerevisiae* copes with toxic metals and metalloids. *FEMS Microbiol Rev* 34(6):925–951. <https://doi.org/10.1111/j.1574-6976.2010.00217.x>
4. Piloni NE, Fernandez V, Videla LA, Puntarulo S (2013) Acute iron overload and oxidative stress in brain. *Toxicology* 314(1):174–182. <https://doi.org/10.1016/j.tox.2013.09.015>
5. Yazgan O, Krebs JE (2012) Mitochondrial and nuclear genomic integrity after oxidative damage in *Saccharomyces cerevisiae*. *Front Biosci (Landmark Ed)* 17:1079–1093. <https://doi.org/10.2741/3974>
6. Herrero E, Ros J, Belli G, Cabisco E (2008) Redox control and oxidative stress in yeast cells. *BiochimBiophysActa* 1780(11):1217–1235. <https://doi.org/10.1016/j.bbagen.2007.12.004>
7. Ballatori N (2002) Transport of toxic metals by molecular mimicry. *Environ Health Perspect* 110(Suppl 5):689–694. <https://doi.org/10.1289/ehp.02110s5689>
8. Jarup L (2003) Hazards of heavy metal contamination. *Br Med Bull* 68:167–182. <https://doi.org/10.1093/bmb/ldg032>
9. Čurko-Cofek B, Grubić Kezele T, Barac-Latas V (2017) Hepsidin and metallothioneins as molecular base for sex-dependent differences in clinical course of experimental autoimmune encephalomyelitis in chronic iron overload. *Med Hypotheses* 107:51–54. <https://doi.org/10.1016/j.mehy.2017.07.022>
10. Bleackley MR, Macgillivray RT (2011) Transition metal homeostasis: from yeast to human disease. *Biometals* 24(5):785–809. <https://doi.org/10.1007/s10534-011-9451-4>
11. Musci G, Polticelli F, Bonaccorsi di Patti MC (2014) Ceruloplasmin-ferroportin system of iron traffic in vertebrates. *World J BiolChem* 5(2):204–215. <https://doi.org/10.4331/wjbc.v5.i2.204>
12. Chen C, Paw BH (2012) Cellular and mitochondrial iron homeostasis in vertebrates. *BiochimBiophysActa* 1823:1459–1467. <https://doi.org/10.1016/j.bbamcr.2012.01.003>
13. Ye H, Rouault TA (2010) Human iron-sulfur cluster assembly, cellular iron homeostasis, and disease. *Biochemistry* 49:4945–4956. <https://doi.org/10.1021/bi1004798>

14. Levi S, Rovida E (2009) The role of iron in mitochondrial function. *BiochimBiophysActa* 1790:629–636. <https://doi.org/10.1016/j.bbagen.2008.09.008>
15. Farina M, Avila DS, da Rocha JB, Aschner M (2013) Metals, oxidative stress and neurodegeneration: a focus on iron, manganese and mercury. *NeurochemInt* 62(5):575–594. <https://doi.org/10.1016/j.neuint.2012.12.006>
16. Kim JJ, Kim YS, Kumar V (2019) Heavy metal toxicity: an update of chelating therapeutic strategies. *J Trace Elem Med Biol* 54:226–231. <https://doi.org/10.1016/j.jtemb.2019.05.003>
17. Matović V, Buha A, Đukić-Čosić D, Bulat Z (2015) Insight into the oxidative stress induced by lead and/or cadmium in blood, liver and kidneys. *Food Chem Toxicol* 78:130–140. <https://doi.org/10.1016/j.fct.2015.02.011>
18. Flora G, Gupta D, Tiwari A (2012) Toxicity of lead: a review with recent updates. *Interdiscip Toxicol* 5:47–58. <https://doi.org/10.2478/v10102-012-0009-2>
19. Eid A, Zawia N (2016) Consequences of lead exposure, and it's emerging role as an epigenetic modifier in the aging brain. *NeuroToxicol* 56:254–261. <https://doi.org/10.1016/j.neuro.2016.04.006>
20. Moteshareh H, Hajikarimlou M, Mulet Indrayanti A, Burnside D, Paula Dias A, Lettl C et al (2018) Heavy metal sensitivities of gene deletion strains for ITT1 and RPS1A connect their activities to the expression of URE2, a key gene involved in metal detoxification in yeast. *PLoS ONE* 13(9):e0198704. <https://doi.org/10.1371/journal.pone.0198704>
21. Hosiner D, Gerber S, Lichtenberg-Frate H, Glaser W, Schüller C, Klipp E (2014) Impact of acute metal stress in *Saccharomyces cerevisiae*. *PLoS ONE* 9(1):e83330. <https://doi.org/10.1371/journal.pone.0083330>
22. Kwolek-Mirek M, Zadrag-Tecza R (2014) Comparison of methods used for assessing the viability and vitality of yeast cells. *FEMS Yeast Res* 14(7):1068–1079. <https://doi.org/10.1111/1567-1364.12202>
23. Wu X, Hasan MA, Chen JY (2014) Pathway and network analysis in proteomics. *J Theor Biol* 362:44–52. <https://doi.org/10.1016/j.jtbi.2014.05.031>
24. Gómez-Serrano M, Camafeita E, Loureiro M, Peral B (2018) Mitoproteomics: tackling mitochondrial dysfunction in human disease. *Oxid Med Cell Longev*. <https://doi.org/10.1155/2018/1435934>
25. Morgenstern M, Stiller SB, Lübbert P, Peikert CD, Dannenmaier S, Drepper F et al (2017) Definition of a high-confidence mitochondrial proteome at quantitative scale. *Cell Rep* 19(13):2836–2852. <https://doi.org/10.1016/j.celrep.2017.06.014>
26. Pagliarini DJ, Calvo SE, Chang B, Sheth SA, Vafai SB, Ong SE et al (2008) A mitochondrial protein compendium elucidates complex I disease biology. *Cell* 134(1):112–123. <https://doi.org/10.1016/j.cell.2008.06.016>
27. Prokisch H, Scharfe C, Camp DG II, Xiao W, David L, Andreoli C et al (2004) Integrative analysis of the mitochondrial proteome in yeast. *PLoS Biol* 2(6):795–804. <https://doi.org/10.1371/journal.pbio.0020160>
28. Pearce DA, Sherman F (1999) Toxicity of copper, cobalt, and nickel salts is dependent on histidine metabolism in the yeast *Saccharomyces cerevisiae* [published correction appears in *J Bacteriol* 1999;181(21):6856]. *J Bacteriol* 181(16):4774–4779
29. Zakrajšek T, Raspor P, Jamnik P (2011) *Saccharomyces cerevisiae* in the stationary phase as a model organism—characterization at cellular and proteome level. *J Proteom* 74(12):2837–2845. <https://doi.org/10.1016/j.jprot.2011.06.026>
30. Jakubowski W, Bartosz W (1997) Estimation of oxidative stress in *Saccharomyces cerevisiae* with fluorescent probes. *Int J Biochem Cell Biol* 29(11):1297–1301. [https://doi.org/10.1016/S1357-2725\(97\)00056-3](https://doi.org/10.1016/S1357-2725(97)00056-3)
31. Zinser E, Daum G (1995) Isolation and biochemical characterization of organelles from the yeast, *Saccharomyces cerevisiae*. *Yeast* 11(6):493–536. <https://doi.org/10.1002/yea.320110602>
32. Čanadi Jurešić G, Blagović B (2011) The influence of fermentation conditions and recycling on the phospholipid and fatty acid composition of the brewer's yeast plasma membranes. *Folia Microbiol* 56(3):215–224. <https://doi.org/10.1007/s12223-011-0040-2>
33. Bradford MM (1976) A rapid and sensitive method for the quantitation of microgram quantities of protein utilizing the principle of protein-dye binding. *Anal Biochem* 72:248–254
34. Gorg A (1991) Two-dimensional electrophoresis. *Nature* 349:545–546. <https://doi.org/10.1038/349545a0>
35. Perkins DN, Pappin DJ, Creasy DM, Cottrell JS (1999) Probability-based protein identification by searching sequence databases using mass spectrometry data. *Electrophoresis* 20(18):3551–3567. [https://doi.org/10.1002/\(SICI\)1522-2683\(19991201\)20:18%3c3551::AID-ELPS3551%3e3.0.CO;2-2](https://doi.org/10.1002/(SICI)1522-2683(19991201)20:18%3c3551::AID-ELPS3551%3e3.0.CO;2-2)
36. The UniProt Consortium (2019) UniProt: a worldwide hub of protein knowledge. *Nucleic Acids Res* 47(D1):D506–D515. <https://doi.org/10.1093/nar/gky1049>
37. Holmes-Hampton GP, Jhurry ND, McCormick SP, Lindahl PA (2012) Iron content of *Saccharomyces cerevisiae* cells grown under iron-deficient and iron-overload conditions. *Biochemistry* 52(1):105–114. <https://doi.org/10.1021/bi3015339>
38. Chen C, Wang J (2007) Response of *Saccharomyces cerevisiae* to lead ion stress. *Appl Microbiol Biotech* 74(3):683–687. <https://doi.org/10.1007/s00253-006-0678-x>
39. Sousa CA, Soares EV (2014) Mitochondria are the main source and one of the targets of Pb (lead)-induced oxidative stress in the yeast *Saccharomyces cerevisiae*. *Appl Microbiol Biotechnol* 98(11):5153–5160. <https://doi.org/10.1007/s00253-014-5631-9>
40. Yuan X, Tang C (1999) DNA damage and repair in yeast (*Saccharomyces cerevisiae*) cells exposed to lead. *J Environ Sci Health Part A* 34(5):1117–1128. <https://doi.org/10.1080/10934529909376885>
41. Millard PJ, Roth BL, Thi HP, Yue ST, Haugland RP (1997) Development of the FUN-1 family of fluorescent probes for vacuole labelling and viability testing of yeasts. *Appl Environ Microbiol* 63(7):2897–2905
42. Van der Heggen M, Martins S, Flores G, Soares EV (2010) Lead toxicity in *Saccharomyces cerevisiae*. *Appl Microbiol Biotechnol* 88:1355–1361. <https://doi.org/10.1007/s00253-010-2799-5>
43. Malina C, Larsson C, Nielsen J (2018) Yeast mitochondria: an overview of mitochondrial biology and the potential of mitochondrial systems biology. *FEMS Yeast Res* 18(5):040. <https://doi.org/10.1093/femsyr/foy040>
44. Shenton D, Smirnova JB, Selley JN, Carroll K, Hubbard SJ, Pavitt GD, Ashe MP, Grant CM (2006) Global translational responses to oxidative stress impact upon multiple levels of protein synthesis. *J Biol Chem* 281(39):29011–29021. <https://doi.org/10.1074/jbc.M601545200>
45. Temple MD, Perrone GG, Dawes IW (2005) Complex cellular responses to reactive oxygen species. *Trends Cell Biol* 15(6):319–326. <https://doi.org/10.1016/j.tcb.2005.04.003>
46. Shenton D, Grant CM (2003) Protein S-thiolation targets glycolysis and protein synthesis in response to oxidative stress in the yeast *Saccharomyces cerevisiae*. *Biochem J* 374:513–519. <https://doi.org/10.1042/BJ20030414>
47. Opalińska M, Meisinger C (2015) Metabolic control via the mitochondrial protein import machinery. *Curr Opin Cell Biol* 33:42–48. <https://doi.org/10.1016/j.ceb.2014.11.001>
48. Justinić I, Katić A, Uršičić D, Čurko-Cofek B, Blagović B, Čanadi Jurešić G (2020) Combining proteomics and lipid analysis to unravel Confidor® stress response in *Saccharomyces cerevisiae*.

- Environ Toxicol 35(3):346–358. <https://doi.org/10.1002/tox.22870>
49. Shi J, Feng H, Lee J, Chen WN (2013) Comparative proteomics profile of lipid-cumulating oleaginous yeast: an iTRAQ-Coupled 2-D LC-MS/MS analysis. PLoS ONE 8(12):e85532. <https://doi.org/10.1371/journal.pone.0085532>
 50. Kim HE, Grant AR, Simic MS, Kohnz RA, Nomura DK, Durieux J et al (2016) Lipid biosynthesis coordinates a mitochondrial-to-cytosolic stress response. Cell 166(6):1539–1552.e16. <https://doi.org/10.1016/j.cell.2016.08.027>
 51. Cadenas E, Davies KJA (2000) Mitochondrial free radical generation, oxidative stress, and aging. Free RadicBiol Med 29(3–4):222–230. [https://doi.org/10.1016/S0891-5849\(00\)00317-8](https://doi.org/10.1016/S0891-5849(00)00317-8)
 52. Ohlmeier S, Kastaniotis A, Hiltunen JK, Bergmann U (2004) The yeast mitochondrial proteome, a study of fermentative and respiratory growth. J BiolChem 279:3956–3979. <https://doi.org/10.1074/jbc.M310160200>
 53. Olin-Sandoval V, Yu JSL, Miller-Fleming L et al (2019) Lysine harvesting is an antioxidant strategy and triggers underground polyamine metabolism. Nature 572:249–253. <https://doi.org/10.1038/s41586-019-1442-6>
 54. Zabriskie TM, Jackson MD (2000) Lysine biosynthesis and metabolism in fungi. Nat Prod Rep 17(1):85–97. <https://doi.org/10.1039/A801345D>
 55. Nielsen J (2019) Yeast cells handle stress by reprogramming their metabolism. Nature 572:184–185. <https://doi.org/10.1038/d41586-019-02288-y>

Publisher's Note Springer Nature remains neutral with regard to jurisdictional claims in published maps and institutional affiliations.